Determination of soil parameters under gravitation and centrifugal forces in 3D infiltration

JOZEF KAČUR
SvF STU Bratislava
Department of Physics
Radlinského 11, 810 05
SLOVAKIA
Jozef.Kacur@fmph.uniba.sk

PATRIK MIHALA
Comenius University Bratislava
Department of Mathematics
Mlynská dolina, 842 48
SLOVAKIA
pmihala@gmail.com

MICHAL TÓTH
Comenius University Bratislava
Department of Mathematics
Mlynská dolina, 842 48
SLOVAKIA
m.toth82@gmail.com

Abstract: A novel set-up for the study of unsaturated flow characteristics in porous media is examined. In this set-up, a sample of cylindrical shape is submerged in water chamber and the water infiltrates into it. The top of the cylinder is isolated and from its bottom water flows out to the collection chamber. Both chambers except of the sample bottom (resp. its part) are mutually isolated. Determination of soil parameters (in fundamental flow characteristics) requires non-invasive measuremets of global characteristics as amount of infiltrated and outflow water in some time moments (see the figure 1 below). When using centrifuge the measurement data could be extended also by measurements of centrifugal force.
A precise and efficient numerical method is developed for solution of mathematical model based on Richard's strongly nonlinear and degenerate equation expressed in terms of van Genuchten/Mualem experimental model describing effective saturation and hydraulic permeability versus pressure. The previously used 1D models (tube shape samples) experience serious issues with the effects of fingering, where due to the small inhomogenities preferable streams in the tube can emerge. Moreover, the isolation of sample mantle is technically difficult, especially in centrifugation mode. On the other hand the numerical realization is much more difficult as in 1D mathematical model. The numerical experiments support our method requiring only simple non-invasive measurements.

Key–Words: water transport, unsaturated porous media, soil parameters, scaling of mathematical model, gravitation and centrifugal forces

1 Introduction

In order to predict the flow and solute transport in soils, the soil hydraulic properties expressed in terms of soil parameters have to be known. These parameters are an input data in the governing mathematical model. This model is expressed in terms of saturation and preasure head in Richard's equation (see (1) below), which is a nonlinear and degenerate parabolic equation with free boundaries between saturated and partially saturated zone and between dry and partially saturated zone. The soil retention and hydraulic permeability functions linking the saturation and preasure head are expressed by means of soil parameters using the Van Genuchten-Mualem ansatz. Determination of soil parameters (via solution of inverse problem) requires very precise solution of direct problem (when all model parameters are known) and additional measurements of inflow/outflow water. In case of centrifugation (the sample with the inflow/outflow chambers are placed in centrifuge arm in horizontal position) we can extend the measuring data adding the values of centrifuge force in prescribed time moments.

Acceleration of data collection can be achieved by using centrifugation. This has been applied in [4] (see also citations there) and [1]. In [4] the equilibrium analysis for a set of rotational speeds has been used to determine soil parameters. The distribution of saturation in equilibria (linked with the corresponding rotational speeds) was measured via electrical signals from electrodes installed in the specimen. Transient measurements have been also applied there. At the beginning the sample was fully saturated and the outflow from the sample was controlled.

In our previous papers [3], [6], [7] we discussed another centrifugation scenario, where non-invasive measurements of flow characteristics have been used and their sufficiency in determining procedure have been demonstrated.

In the present contribution we focus on gravitational driving force and the centrifugation will be sketched only. Unlike in previous papers, we consider more realistic 3D rotationally symmetric sample.

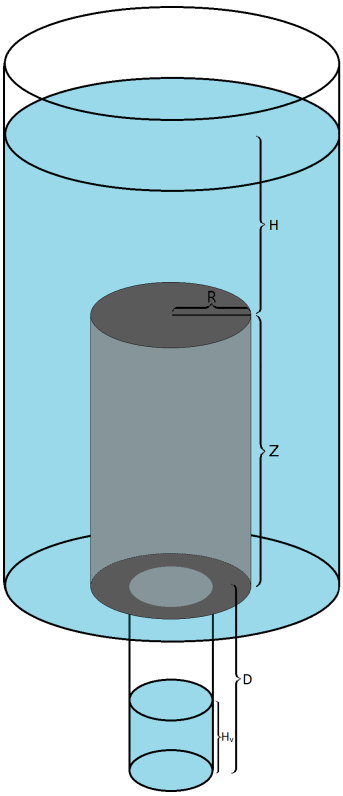

Figure 1: Sample

2 Mathematical model

Our sample is a cylinder with radius R and height Z. We transform the mathematical model using cylindrical coordinates (r, z). Then the governing PDE for infiltration reads as follows

$$\partial_t \theta(h) = \frac{1}{r}\partial_r(rK(h)\partial_r h) + \partial_z(K(h)(\partial_z h - \beta)) \quad (1)$$

where the saturation θ, depending on pressure head h, is of the form

$$\theta(h) = \theta_r + (\theta_s - \theta_r)\theta_{ef}(h), \quad (2)$$

with irreducible saturation θ_r, porosity θ_s and effective saturation $\theta_{ef}(h)$. We consider the fundamental saturation-pressure law in terms of van Genuchten-Mualem empirical ansatz ($h \leq 0$ in unsaturated zone, in saturated zone $\theta_{ef} = 1$, $h > 0$)

$$\theta_{ef}(h) = \frac{1}{(1 + (\alpha h)^n)^{\frac{1}{m}}}, \quad (3)$$

where $\alpha,\ n,\ m = 1 - \frac{1}{n}$ are soil parameters. The hydraulic permeability $K = K(h)$ is in van Genuchten-Mualem ansatz

$$K(h) = K_s\,(\theta_{ef}(h))^{\frac{1}{2}} \cdot \left(1 - (1 - (\theta_{ef}(h))^m)^{\frac{1}{m}}\right)^2, \quad (4)$$

where K_s (also soil parameter) is a hydraulic permeability for saturated porous media, i.e., $K_s = K(0)$. In the gravitational mode $\beta = 1$ and in the centrifugation mode (coordinate z is in the direction of centrifuge arm) we have

$$\beta = \frac{\omega^2}{g}(L - z)$$

where L is the distance of sample bottom from the centrifugation axis. The flux in cylindrical coordinates is of the form

$$\mathbf{q} = -(q_r, q_z)^T, \quad (5)$$
$$q_r = K(h)\partial_r h,\ q_z = K(h)(\partial_z h - \beta)$$

We note that our model includes both saturated (elliptic PDE) and unsaturated (parabolic PDE) zones. We consider initially (at $t = 0$) the dry sample $h = -\infty$), but in the numerical experiments we use $h = -10^4$. The top of our sample $\Gamma_{top} = \{r \in (0, R), z = Z\}$ is isolated, i.e., we consider $q_z = 0$ and the same condition we consider on the part $\{r \in (R1, R), z = 0\}$ of the bottom. Through the part $\Gamma_{out} = \{r \in (0, R1), z = 0\}$ the infiltrated water can outflow to the collection chamber, i.e. we consider $\partial_z h = 0$ on Γ_{out} in q_z (see (5)). The boundary condition on the sample mantel $\Gamma_{mant} = \{r = R, z \in (0, Z)\}$ reflects the hydrostatic pressure generated by water level $H(t) \geq 0$ (measured from the top of the sample) at the coordinate $0 \leq z \leq Z$. Then our boundary condition on Γ_{mant} is

$$h(t, R, z) = H(t) + (Z - z) \quad (6)$$

Due to the mass ballance argument, the change in $H(t)$ reflects the infiltration flux through Γ_{mant} for $t > 0$. Thus, our system is closed by ODE

$$\dot{H}(t) = -Q \int_{\Gamma_{mant}} q_z\, d\Gamma_{mant} \quad (7)$$

where Q is the ratio of the areas of Γ_{top} and the crossection of inflow chamber. The amount of outflow water in the collection chamber is given by

$$M_{out}(t) = \int_0^t \int_{\Gamma_{out}} q_z\, d\Gamma_{out})dt$$

which coud be expressed in terms of water level

$$H_{out}(t) = Q_1 M_{out}(t)$$

where Q_1 is the ratio of areas $\Gamma_(out)$ of the crossection area and collection area of the collection chamber.

In the case of centrifugation, the condition (6) is replaced by

$$h(t, R, z) = \int_z^{H(t)+Z} \frac{\omega^2}{g}(L - p)dp.$$

3 Numerical method

Our correct and efficient numerical method in 1D substantially used mathematical model (in terms of ODE) describing the interfaces between fully, partially saturated and dry zones of the sample. In the more dimensional case we do not have such information. Therefore more discretization grid points have to be used. We apply devised linearization and regularization to manage serious difficulties concerning degeneracy and strong nonlinearities appearing in a small neighbourhood of mentioned interfaces. The solution has very sharp, moving front between partially saturated and dry zones.

We have developed two different approximation schemes. After space discretization (based on finite volume method) we reduce our system to the ODE system. In fact, the obtained ODE system is singular and some regularization was applied. On the other hand all nonlinearities are approximated correctly. In the second scheme we follow the idea in Celia [5], which also was applied in the well known software HYDRUS [2]. The nonlinearities are approximated by a appropriate iteration procedure of linearized system (Quasinewton method). Both methods give nearly the same results, but the second one is much quicker and therefore is more suitable for solving inverse problems.

3.1 Approximation of governing equations

Consider the grid points $(r_i, z_l) = (i\Delta r,\ l\Delta z)$ for $i \in \left\{0, 1, \dots, \frac{R}{\Delta r}\right\}$ and $l \in \left\{0, 1, \dots, \frac{Z}{\Delta z}\right\}$ with the fixed space step $(\Delta r, \Delta z)$ and flexible time step Δt_j which will be modified in the iteration procedure. To construct approximation scheme linked with the grid point (r_i, z_l, t_{j+1}), we integrate (1) over the volume

$$V_{i,l,j} = ((r_i - \frac{\Delta r}{2},\ r_i + \frac{\Delta r}{2})\times$$

$$(z_l - \frac{\Delta z}{2},\ z_l + \frac{\Delta z}{2}) \times (t_j,\ t_j + \Delta t_j).$$

We apply integration by parts in corresponding terms and approximate

$$\partial_x h(r_{i+1/2,z_l,t_j}) \approx \frac{h(r_i+1, z_l, t_j) - h(r_i, z_l, t_j)}{\Delta r}$$

and

$$h(r_{i+1/2,z_l,t_j}) \approx \frac{h(r_i+1, z_l, t_j) + h(r_i, z_l, t_j)}{2}.$$

Similarly we approximate

$$\partial_r h(r_{i-1/2,z_l,t_j}),\ h(r_{i-1/2,z_l,t_j}).$$

In the same way we approximate $\partial_z h$ and the values of $K(h)$ in the middle grid points, where the average of values h in neighbouring grid points is used. Then our approximation scheme reads as follows

$$\frac{(\theta_{i,l}^{j+1} - \theta_{i,l}^{j})}{\Delta t_j} = \frac{r_{i+\frac{1}{2}}}{r_i} K_{i+\frac{1}{2},l}^{j+1} \frac{h_{i+1,l}^{j+1} - h_{i,l}^{j+1}}{(\Delta r)^2} - \quad (8)$$

$$\frac{r_{i-\frac{1}{2}}}{r_i} K_{i-\frac{1}{2},l}^{j+1} \frac{h_{i,l}^{j+1} - h_{i-1,l}^{j+1}}{(\Delta r)^2} +$$

$$\frac{1}{\Delta z}\left(K_{i,l+\frac{1}{2}}^{j+1}\left(\frac{h_{i,l+1}^{j+1} - h_{i,l}^{j+1}}{\Delta z} - 1\right) -\right.$$

$$\left. K_{i,l-\frac{1}{2}}^{j+1}\left(\frac{h_{i,l}^{j+1} - h_{i,l-1}^{j+1}}{\Delta z} - 1\right)\right).$$

This is strongly nonlinear system because of (3). We linearize it by means of quasinewton iterations with iteration parameter k (see [5]). The left hand part in (8) we linearize by

$$\frac{\left(\theta_{i,l}^{j+1,k+1} - \theta_{i,l}^{j}\right)}{\Delta t_j} = \quad (9)$$

$$C_{i,l}^{j+1,k} \frac{h_{i,l}^{j+1,k+1} - h_{i,l}^{j+1,k}}{\Delta t_j} + \frac{\left(\theta_{i,l}^{j+1,k} - \theta_{i,l}^{j}\right)}{\Delta t_j} \equiv$$

$$L_{i,l}^{j+1,k}$$

where

$$C_{i,l}^{j+1,k} = \left(\frac{\mathrm{d}\theta}{\mathrm{d}h}\right)^{j+1,k}.$$

In the right hand side in (8) we consider the values $h^{j+1,k}$ (from previous iteration step) in $K(h)$. Our linearization reads as follows

$$L_{i,l}^{j+1,k} =$$

$$\frac{r_{i+\frac{1}{2}}}{r_i} K_{i+\frac{1}{2},l}^{j+1,k} \frac{h_{i+1,l}^{j+1,k+1} - h_{i,l}^{j+1,k+1}}{(\Delta r)^2} - \quad (10)$$

$$\frac{r_{i-\frac{1}{2}}}{r_i} K_{i-\frac{1}{2},l}^{j+1,k} \frac{h_{i,l}^{j+1,k+1} - h_{i-1,l}^{j+1,k+1}}{(\Delta r)^2} +$$

$$\frac{1}{\Delta z}\left(K_{i,l+\frac{1}{2}}^{j+1,k}\left(\frac{h_{i,l+1}^{j+1,k+1} - h_{i,l}^{j+1,k+1}}{\Delta z} - 1\right) -\right.$$

$$\left. K_{i,l-\frac{1}{2}}^{j+1,k}\left(\frac{h_{i,l}^{j+1,k+1} - h_{i,l-1}^{j+1,k+1}}{\Delta z} - 1\right)\right).$$

Thus (9),(10) represent a linear algebraic system in terms of $h_{i,l}^{j+1,k+1}$. The iteration will stop for $k = k^*$ when

$$||\mathbf{h}^{j+1,k+1} - \mathbf{h}^{j+1,k}|| < tollerance.$$

Then we put $\theta_{i,l}^{j+1} = \theta_{i,l}^{j+1,k^*}$ corresponding to $h_{i,l}^{j+1,k^*}$ (see (3)). The same approximation strategy we use at boundary points where the controll volume $V_{i,l,j}$ is reduced.

3.2 Numerical acceleration

The computational process can be significantly accelerated by a suitable choice of time step and starting value $\mathbf{h}^{k=0}$. Starting point can be constructed via interpolation of few (cca 5) values from previous time steps of $\mathbf{h}$.

Additional speed increase can be reached by damping technique and appropriate choice of time step depending on the number of iterations in previous iteration procedure. We have to note (and it is very surprising) that by suitable choice of previous atributes in iteration procedure it is possible to reach significant reduction in the computational time. Without damping the iteration process can even fail.

3.3 Approximation by ODE system

We construct the governing ODE linked with the grid point (r_i, z_l) (similarly as before) integrating (1) over controll volume

$$V_{i,l} = ((r_i - \frac{\Delta r}{2},\ r_i + \frac{\Delta r}{2})\times$$

$$(z_l - \frac{\Delta z}{2},\ z_l + \frac{\Delta z}{2}).$$

The left hand side of (1) we approximate (in (r_i, z_l)) by

$$\frac{\partial \theta_{i,l}(t)}{\partial h_{i,l}(t)} \partial_t h_{i,l}(t) \Delta r \Delta z$$

and the right hand side in (1) we approximate using integration by parts similarly as before. Then we obtain a nonlinear ODE system of the form

$$M(t, \mathbf{h}) \frac{d\mathbf{h}}{dt} = \mathbf{F}(t, \mathbf{h})$$

which can be solved by (proffesional) solver for stiff ODE. In fact matrix M should be regularized, because it degenerates (in saturated zone $\theta(t) = \theta_s$). Becuse of the degeneracy the computing time is significantly increased. Moreover, the ODE system is large.

Figure 2: Pressure at $t = 20$.

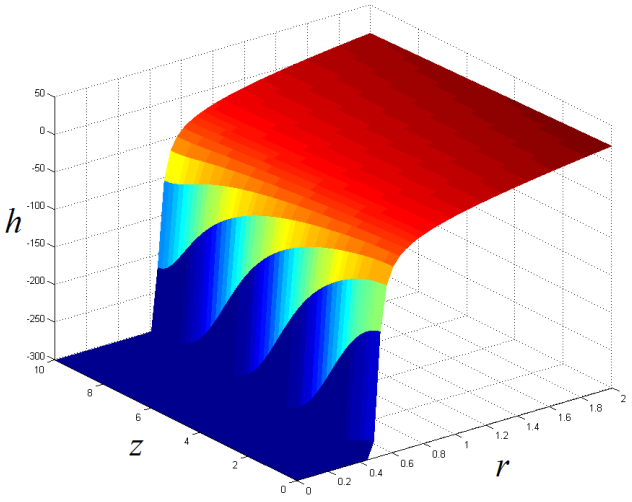

3.4 Numerical experiments

The "standard" model data used in numerical experiments are:

$$Z = 10,\ R = 2,\ H(0) = 5,\ R_1 = 1,$$

$$\alpha = -0.0189,\ n = 2.81,\ (m = 1 - \frac{1}{n}),$$

$$K_s = 2.4 \times 10^{-4},\ \theta_r = 0.02,\ \theta_s = 0.38.$$

Figure 2 express pressure h graphically at a time moment $T = 20$. Very similar picture can be obtained by plotting effective saturation θ instead of pressure h (see (3)). We can see the sharp front of infiltrated water. This moving front causes numerical difficulties. Our solution should be precise enough to enable solving the inverse problem. The figure 3 (blue color) depicts time evolution of $H(t)$ and time evolution of the outflow $3000 M_{out}(t)$.

4 Solution of the inverse problem

In the solution of the inverse problem we minimize the discrepancy between the measured and computed data. Minimization problem is solved in an iterative way using well known solver *fminsearch* from the MATLAB toolbox. At solving inverse problems determining soil parameters $(\alpha,\ n,\ K_s)$ we consider starting points different from standard data.

In the experiment below we demonstrate applicability of our method in determining soil parameters. Firstly we prepare standard data $H(t)$ and $M_{out}(t)$ in 50 uniformly distributed time sections in the observation interval $[0.5, 25]$. Then using random function we add 5% noise to our data. Then the noised data are sorted, because the nature of the experiment dictates

Figure 3: Standard and noised data

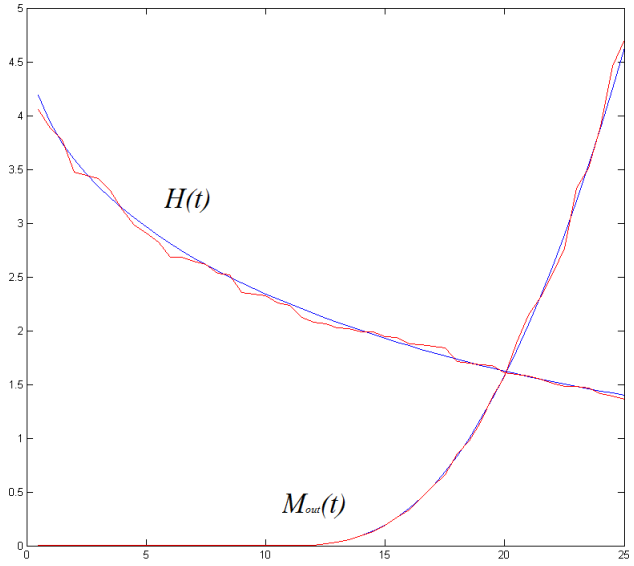

that data are monotonous. This will represent measuring data. The figure 3 shows standard data (blue) and noised data (red). The optimal parameters of inverse problems using this measured data are in the first pair of rows in table 1.

Secondly, we "forget" standard soil parameters and use different starting points for them. As a result of the inverse procedure (by minimization of discrepancy between measured and computed data) we obtain "optimal" solution. Our starting points consist of all combinations of parameters

$$\alpha \in \{-0.017,\ -0.02\},$$
$$n \in \{2.6, 3\},$$
$$K_s \in \{2 \times 10^{-4}, 2.8 \times 10^{-4}\}.$$

The parameter K_s can be determined distinctively by simple experiment with fully saturated sample. Therefore we also solved inverse problems for only 2 parameters α, n assuming $K_s = 2.4 \times 10^{-4}$.

In both cases the optimal solution does not depend on the choice of a starting point (the relative differences are less then 10^{-5}). However, the small dependance on noise generation is observed. The table 1 shows optimal parameters for different noises. The pairs of succesive rows correspond to the standard data with the same noise. In each pair, the second row represents a solution of inverse problem with only 2 parameters.

5 Conclusion

Numerical experiments demonstrate efficiency of our numerical method also in more dimensional case using only non-invasive measurements. The 5% noise

Table 1: Optimal parameters with 3 different noises

α	n	$K_s \times 10^4$
-0.015359	2.7636	2.168
-0.018427	2.7077	
-0.018163	2.9865	2.310
-0.019119	2.8467	
-0.019417	2.7421	2.446
-0.018907	2.8037	

in our measurements effects the $5-6\%$ defect in case with two soil parameters $\alpha,\ n$. In the case with 3 soil parameters the defect reaches up to 15%. During series of experiments we have remarked very low dependance of optimal solution on starting points. Greater dependance is linked to the type of generated noise.

We expect (on the base of our experiences with 1D model) that application of our method in a centrifugation mode will produce even more precise results in solving inverse problems. The reason is, that the saturation distribution in the sample and in output can produce more dynamical change. Moreover, third important information can be obtained by measuring time evolution of centrifugal force. This have been implemented in our previous centrifuge version in 1D (see [3]). The outflow water significantly changes the centrifugal force, especially when D is large (see figure 1). Moreover, it is possible to change the rotational speed during centrifugation, which also significantly influences the solution.

Acknowledgements: The authors confirm support by the Slovak Research and Development Agency APVV-15-0681 and VEGA 1/0565/16.

References:

[1] GK D. Constales, J. Kacur: Determination of soil parameters via the solution of inverse problems in infiltration. Computational Geosciences 5 (2004), p. 25-46.

[2] J. Šimunek, M. Šejna, H. Saito, M. Sakai, M. Th. van Genuchten: The Hydrus-1D Software Package for Simulating the Movement of Water, Heat, and Multiple Solutes in Variably Saturated Media. 2013.

[3] J. Kačur, B. Malengier, P. Kišon: A numerical model of transient unsaturated flow under centrifugation based on mass balance. Transport in Porous Media: Vol.87,3, (2011), p. 793-813.

[4] J. Šimunek, J. R. Nimo: Estimating soil hydraulic parameters from transient flow experi-

ments in a centrifuge using parameter optimization technique. Water Resour. Res. 41, W04015 (2005).

[5] M. A. Celia, Z. Bouloutas: A general mass-conservative numerical solution for the unsaturated flow equation. Water Resour. Res. 26 (1990), p. 1483-1496.

[6] J.Kačur,B.Malengier,P.Kišon: Unsaturated-saturated flow in porous media under centrifugation. Numerical analysis of Heat and Mass Transfer in Porous Media, Berlin,Springer,(2012), p. 275-295.

[7] 4. J.Kačur, J.Minar, H.Budačova :Determination of soil parameters based on mathematical modelling of centrifugation. In International Journal of Mathematical Modelling and Numerical Optimisation, vol. 5, no.3,(2014,) p. 153-170.